

# Accepted Manuscript

New selective cyclooxygenase-2 inhibitors from cyclocoumarol: Synthesis, characterization, biological evaluation and molecular modeling

Anita Rayar, Nathalie Lagarde, Frederique Martin, Florent Blanchard, Bertrand Liagre, Clotilde Ferroud, Jean-François Zagury, Matthieu Montes, Maité Sylla-Iyarreta Veitia



PII: S0223-5234(18)30067-9

DOI: [10.1016/j.ejmech.2018.01.054](https://doi.org/10.1016/j.ejmech.2018.01.054)

Reference: EJMECH 10131

To appear in: *European Journal of Medicinal Chemistry*

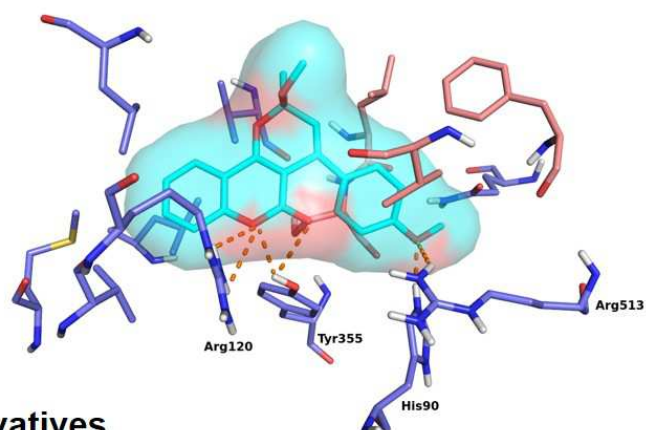
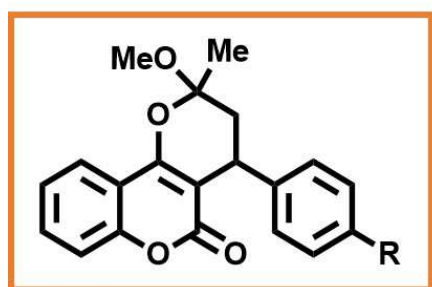
Received Date: 12 October 2017

Revised Date: 26 December 2017

Accepted Date: 16 January 2018

Please cite this article as: A. Rayar, N. Lagarde, F. Martin, F. Blanchard, B. Liagre, C. Ferroud, Jean.-Franç. Zagury, M. Montes, Maité. Sylla-Iyarreta Veitia, New selective cyclooxygenase-2 inhibitors from cyclocoumarol: Synthesis, characterization, biological evaluation and molecular modeling, *European Journal of Medicinal Chemistry* (2018), doi: 10.1016/j.ejmech.2018.01.054.

This is a PDF file of an unedited manuscript that has been accepted for publication. As a service to our customers we are providing this early version of the manuscript. The manuscript will undergo copyediting, typesetting, and review of the resulting proof before it is published in its final form. Please note that during the production process errors may be discovered which could affect the content, and all legal disclaimers that apply to the journal pertain.



**Cyclocoumarol derivatives**  
**Selective COX-2 inhibitors**

ACCEPTED MANUSCRIPT

## New selective cyclooxygenase-2 inhibitors from cyclocoumarol: synthesis, characterization, biological evaluation and molecular modeling

Anita Marie Rayar <sup>a, b</sup>, Nathalie Lagarde <sup>b</sup>, Frederique Martin<sup>c</sup>, Florent Blanchard<sup>d</sup>, Bertrand Liagre <sup>c</sup>, Clotilde Ferroud <sup>a</sup>, Jean-François Zagury <sup>b</sup>, Matthieu Montes <sup>b</sup>, Maité Sylla-Iyarreta Veitia<sup>a\*</sup>

<sup>a</sup> *Equipe de Chimie Moléculaire du Laboratoire CMGPCE, EA 7341, Conservatoire national des arts et métiers, 2 rue Conté, 75003, Paris*

<sup>b</sup> *Laboratoire Génétique Bioinformatique et Applications, EA 4627, Conservatoire National des Arts et Métiers, 2 rue Conté, 75003 Paris.*

<sup>c</sup> *Laboratoire de Chimie des Substances Naturelles, EA1069, Faculté de Pharmacie, 2 rue du Dr Marcland, 87025 Limoges.*

<sup>d</sup> *Institut de Chimie des Substances Naturelles, CNRS UPR 2301, Université. Paris-Sud, Université Paris-Saclay, Gif-sur-Yvette, France.*

Corresponding author:

*E-mail address* : [maite.sylla@lecnam.net](mailto:maite.sylla@lecnam.net) (M. Sylla-Iyarreta Veitia)

### ABSTRACT

In this work, a serie of cyclocoumarol derivatives was designed, synthesized, characterized and studied for their potentialities as selective inhibitors of COX-2. All target compounds have been screened for their anti-inflammatory activity by the assay of PGE<sub>2</sub> production. Among them, compound **5d** exhibited the most potent inhibitory activity with a PGE<sub>2</sub> inhibition compared to NS-398 (79% and 88% respectively) and showed non-inhibitory activity towards the COX-1 enzyme. Docking studies revealed the capacity of this compound to occupy the selective COX-2 cavity establishing additional hydrogen bonds between the oxygen of the methoxy group and the His90 and Arg513 of the binding site of the enzyme.

**Keywords** : Anti-inflammatory, COX-2 inhibitors, COX-1/COX-2 inhibition, Cyclocoumarol, Cyclooxygenase, Docking study

## 1- Introduction

Inflammation is a complex phenomenon affecting millions of people around the world and is involved in the development of many human diseases. The inflammatory response is controlled by a wide variety of mediators, including prostaglandins (PGs), which play a major role in the inflammatory response mediated by cyclooxygenases. The inhibition of these inflammatory mediators can treat the disease, reduce the inflammation but lead to undesirable side effects [1]. Therefore, the development of new anti-inflammatory drugs represents a real challenge considering the benefit-risk balance as one of major concerns in therapeutics.

Cyclooxygenase-2 (COX-2) is a key enzyme involved in the inflammation process particularly in the conversion of arachidonic acid to prostanoids [2, 3]. Non-steroidal anti-inflammatory drugs (NSAID) act as selective COX-2 inhibitors by specifically targeting COX-2. Several NSAID have been developed and approved for commercial use (Fig. 1). Nonetheless clinical trials revealed that despite the reduction of intestinal disorders these inhibitors cause significant cardiovascular, liver and allergic problems resulting in the withdrawal of certain compounds from the market [4, 5].

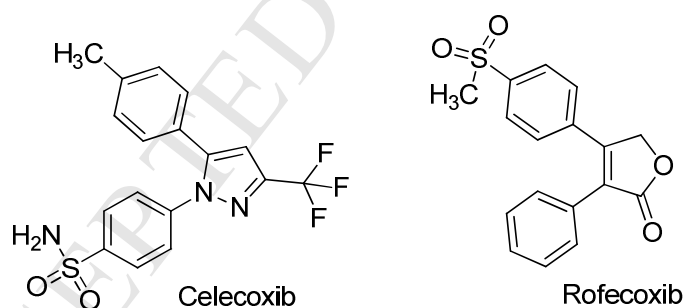


**Fig. 1.** Commercially available COX-2 inhibitors used to treat inflammation

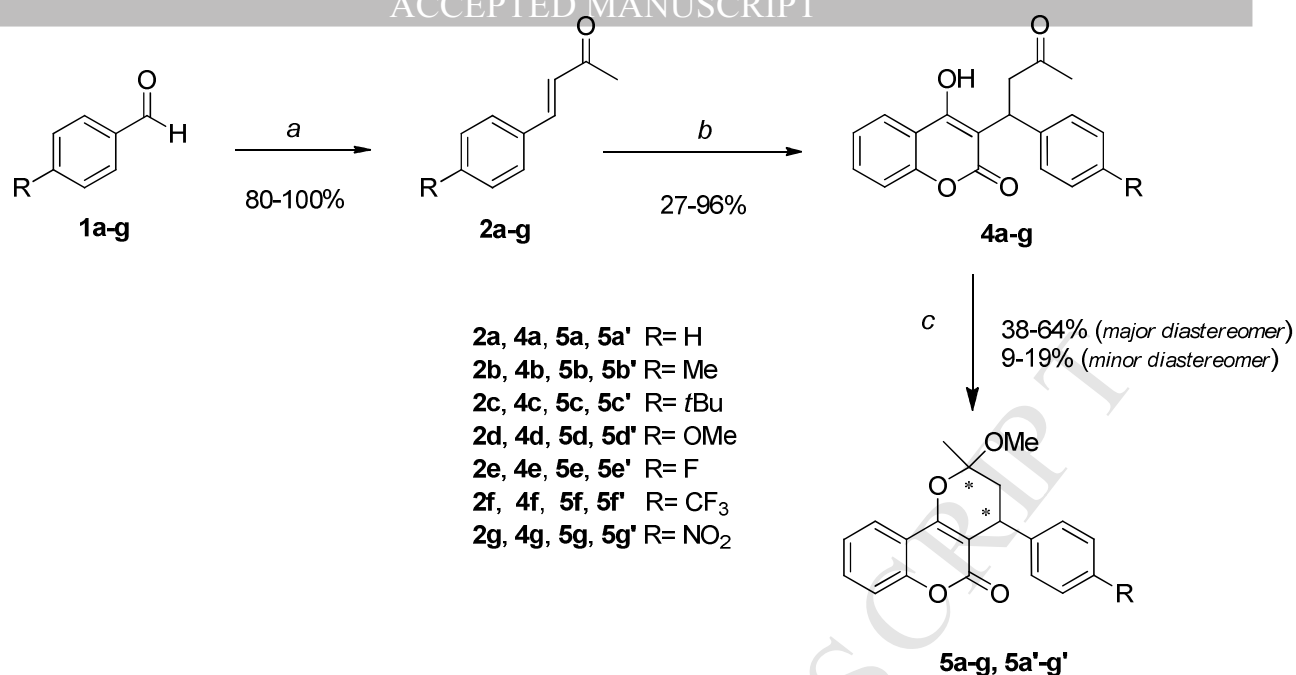
In a previous study, the cyclocoumarol, an anticoagulant drug, was identified as a potential anti-inflammatory compound by TOMOCOMD-CARDD method. The *in silico* results were confirmed by biological studies using a zebrafish model [6]. Based on these observations and in an attempt to pursue the development of new anti-inflammatory agents potentially COX-2 selective inhibitors, a series of novel cyclocoumarol derivatives was designed. We hereby report the synthesis and spectroscopic characterization of these derivatives. The X-ray crystallographic structural analysis is also described. The prepared compounds were evaluated for their inhibitory activity on COX-2 and compared with a

recognized selective COX-2 inhibitor, NS-398. The selectivity for COX-1 and COX-2 isozymes has also been evaluated. To our knowledge, the biological evaluation of COX-2 inhibitory activity of these compounds is related herein for the first time. Additionally, molecular docking studies were carried out to understand the binding modes of these new compounds to the active site of COX-2.

## 2. Results and discussion

### 2.1 Chemistry

The synthetic strategy used to prepare the target compounds **5a-g**, **5a'-g'** is outlined in Scheme 1. The key intermediates, benzalacetones **1a-g**, were synthesized from acetone and the corresponding aldehyde in the presence of aqueous NaOH solution under microwave activation. This optimized procedure has been previously described [7]. The functionalized warfarin derivatives **4a-g** were prepared by 1.4 Michael addition, coupling an equimolar of 4-hydroxycoumarin **3** and the corresponding benzalacetones **2a-g** under reflux in water [8]. Inspired by Barker *et al.* protocol [9] the experimental conditions were optimized by adding 0.05 equiv. of *N, N* diisopropylethylamine (DIPEA) as catalyst. Warfarin intermediates were isolated in yields between 27% and 96% with reaction times among 4- 48 h. To our knowledge, the use of DIPEA in water, has never been described in literature to prepare warfarin analogues *via* 1.4 Michael addition (See Supplementary data). It should be noticed that the low yield of 27% obtained for compound **4e** could be explained by a laborious workup.



**Scheme 1.** Synthesis of cyclocoumarol derivatives (**5a-g**), (**5a'-g'**) (a): Aldehyde (1 equiv), acetone (13.6 equiv), NaOH (0.6 g / cm<sup>3</sup> of water), microwaves irradiation (40/50 °C, 5 W, 10-15 min.); (b): Hydroxycoumarin (**3**) (1 equiv), DIPEA (5% mole), water [0,6 M], reflux, 4-48 h; (c): HCl 4% MeOH (10 equiv), reflux, 22-66 h.

Compounds **5a-g** and **5a'-g'** were prepared by cyclisation of corresponding functionalized warfarins **4a-g**. Heating at reflux of compounds **4a-g** in methanolic HCl 4% afforded, the desired pyranocoumarins **5a-g** and **5a'-g'** with reaction times among 22-66 h. Then, purified by flash chromatography major diastereomers **5a-g** were obtained in yields between 38% and 64% and minor diastereomers **5a'-g'** were isolated in yields of 9-19%. The structures of stereoisomers were confirmed by <sup>1</sup>H NMR and X-ray crystallographic analysis.

## 2.2 <sup>1</sup>H NMR and X-ray diffraction analysis

The <sup>1</sup>H NMR spectra of cyclocoumarol derivatives **5a-g**, **5a'-g'** exhibited characteristic signals allowing an easy distinction between the major and the minor diastereomers. To illustrate this, the proton correlation have been confirmed by 2D NMR (Fig. 2 and 3).

The major diastereomer **5a**, displayed an ABX system where diastereotopic protons H13eq (2.52 ppm) and H13ax (2.01 ppm) were coupled with the benzylic proton in axial position, Hax (4.16 ppm). The protons H13eq and H13ax were coupled with a geminal coupling constant value of 14.0 Hz and the benzylic proton was coupled with protons H13eq and H13ax with a coupling constant of 6.9 and 11.8 Hz respectively, (Fig. 2).

Chemical Shift in ppm	Structural information
1.70 (s, 3H);	C <sub>21</sub> -H
2.01 (dd, 1H, , $J_{gem} = 14.0$ Hz, $J_{13ax-14ax} = 11.8$ Hz );	C <sub>13ax</sub> -H
2.52 (dd, 1H, H13eq, $J_{gem} = 14.0$ Hz, $J_{eq-ax} = 6.9$ Hz );	C <sub>13eq</sub> -H
3.36 (s, 3H,);	C <sub>22</sub> -H
4.16 (dd ,1H, $J_{ax-ax} = 11.8$ Hz, $J_{ax-eq} = 6.9$ Hz );	C <sub>14ax</sub> -H
7.24-7.26 (m, 2H);	C <sub>16</sub> -H, C <sub>20</sub> -H
7.28-7.35 (m, 5H);	C <sub>6</sub> -H, C <sub>8</sub> -H, C <sub>17</sub> -H, C <sub>18</sub> -H, C <sub>19</sub> -H
7.53-7.58 (ddd, 1H, $J = 9.4, 7.4, 1.7$ Hz);	C <sub>7</sub> -H
7.91 (dd, 1H, $J = 8.0, 1.3$ Hz);	C <sub>5</sub> -H

**Fig. 2.** Protons correlations and chemical shift values of major diastereomer of cyclocoumarol **5a** by 2D NMR.

The minor diastereomer **5a'** exhibited a typical coupling constant of a benzylic proton in equatorial position. The Heq at 4.19 ppm was coupled with the two diastereotopic protons H13eq and H13ax with coupling constants of 3.7 and 7.2 Hz respectively. The proton H13ax (2.38 ppm) was coupled with H13eq (2.52 ppm) with a geminal coupling constant of 14.1 Hz, (Fig. 3).

Chemical Shift in ppm	Structural information
1.69 (s, 3H);	C <sub>21</sub> -H
2.38 (dd, 1H, $J_{gem} = 14.0$ Hz, $J_{13ax-14eq} = 7.4$ Hz );	C <sub>13ax</sub> -H
2.52 (dd, 1H, H13eq, $J_{gem} = 14.1$ Hz, $J_{eq-eq} = 3.8$ Hz );	C <sub>13eq</sub> -H
3.29 (s, 3H,);	C <sub>22</sub> -H
4.19 (dd ,1H, $J_{eq-ax} = 7.2$ Hz, $J_{eq-eq} = 3.7$ Hz );	C <sub>14eq</sub> -H
7.21-7.32 (m, 5H);	C <sub>16</sub> -H, C <sub>17</sub> -H, C <sub>18</sub> -H, C <sub>19</sub> -H, C <sub>20</sub> -H
7.34-7.43 (m, 2H);	H
7.60-7.62 (m, 1H,);	C <sub>6</sub> -H, C <sub>8</sub> -H
7.96 (dd, 1H, $J = 7.8, 1.2$ Hz);	C <sub>7</sub> -H
	C <sub>5</sub> -H

**Fig.3.** Protons correlations and chemical shift values of minor diastereomer of cyclocoumarol **5a'** by 2D NMR.

Crystallography studies of 2-methoxy-2-methyl-4-phenyl-3,4-dihydropyrano[3,2-c]chromen-5(2H)-one (**5a** and **5a'**) and 2-methoxy-2-methyl-(1-(4-methoxyphenyl))-3,4-dihydropyrano[3,2-c]chromen-5(2H)-one (**5d**) were performed at room temperature on a Rigaku XtalabPro diffractometer equipped with a microfocus source (MicroMax003\_Mo) and multilayer confocal mirrors (Mo K $\alpha$  radiation,  $\lambda = 0.71075$  Å). The crystal and structure refinement data of compounds **5a**, **5a'** and **5d** are reported in the supplementary data.

The crystallographic structure of the two diastereomers couples of cyclocoumarol **5a** and **5a'** were in agreement with the literature[10] and confirmed that cyclocoumarol could be exist in the form of a pair of diastereomers: (12*S*,14*S*)/(12*R*,14*R*) and (12*S*,14*R*)/(12*R*,14*S*).

In a solid state, minor diastereomer **5a'** (12*S*,14*R*)/(12*R*,14*S*) form a preferred half-chair conformation in which the methoxy and phenyl groups are axially and pseudoaxially positioned respectively. This unusual spatial rearrangement could be explained by a close nonbonded contact between the carbone 15 and the oxygen atom of ketal function of 2.923(2) Å. The relative stability of this conformation reflects the dipole interactions of the oxygens bonded to the ketal carbon and is comparable with the anomeric effect observed in glycosides [10] (Fig. 4).

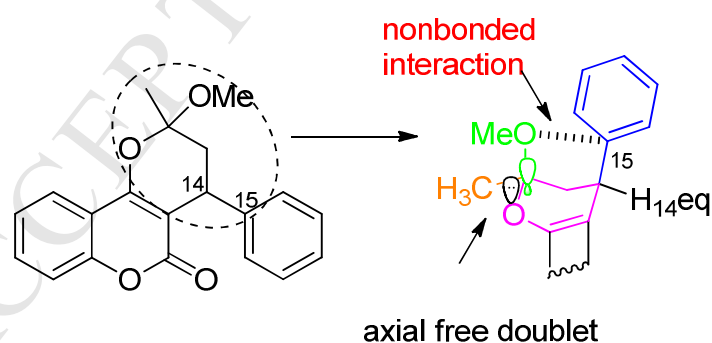


**Fig. 4.** Representation of the proposed spatial rearrangement of minor diastereomer of **5a**.

For major diastereomer **5a**, containing the enantiomers couples (12*S*,14*S*)/(12*R*,14*R*), only the half-chair conformation, in which the methyl and phenyl groups are equatorial and pseudoequatorial respectively is consistent with the values of the coupling constants determined by  $^1\text{H}$  NMR (See experimental section). Since compound **5a** possess the all-staggered conformation in which no obvious nonbonded

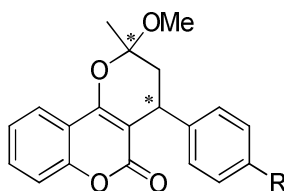
interactions occur between the oxygen bonded to the ketal carbon and the carbone 15, it is the most realistic conformation based on steric and dipole effects.

### 2.3 Biological evaluation of cyclocoumarol analogues

The inhibitory activity on COX-2 was evaluated by determination of the PGE<sub>2</sub> production inhibition, the prostaglandin predominantly overproduced in case of inflammation. The synthesis of PGE<sub>2</sub> was evaluated after pretreatment with the compounds at 10 μM for 2 h and then treatment with LPS (10 ng/mL) for 24 h. The Raw 264.7 cells were seeded at 2.10<sup>5</sup> cells / well for 24 h and then processed as described in the experimental section. PGE<sub>2</sub> levels were determined from the culture supernatants using an EIA kit (Cayman Chemical). The results are expressed as the mean ± SD of independent experiments. NS-398, a specific inhibitor of COX-2, was used as a reference [11] (Table 1 and Fig. 5).

All the synthesized cyclocoumarol derivatives exhibited an inhibitory activity of about 50% inhibition (**5a**, **5b**, **5c**, **5e**). The compound **5d** bearing a methoxy group displayed the strongest inhibition of PGE<sub>2</sub> synthesis compared to the reference NS-398 (79% and 88% inhibition respectively). However, introduction of electro-withdrawing groups trifluoromethyl and nitro (compound **5f** and **5g**) led to a significant decrease of inhibitory activity of COX-2 (31% and 0% inhibition respectively). Minor diastereomers were also evaluated and displayed lower inhibiting activities compared to their corresponding major isomers (Table 1 and Fig. 5).

**Table 1:** Inhibition of PGE<sub>2</sub> production stimulated by LPS by pharmacological agents in the Raw 264.7 cells (compared with NS-398 used as reference, 88% of inhibition)



Compounds	R	% inhibition of PGE <sub>2</sub>
<b>5a</b> ( <b>5a'</b> )	H	50 (27)
<b>5b</b> ( <b>5b'</b> )	CH <sub>3</sub>	60 (30)
<b>5c</b> ( <b>5c'</b> )	<i>t</i> -Bu	52 (45)

<b>5d (5d')</b>	OMe	79 (nd)
<b>5e (5e')</b>	F	48 (14)
<b>5f (5f')</b>	CF <sub>3</sub>	31 (4)
<b>5g (5g')</b>	NO <sub>2</sub>	0

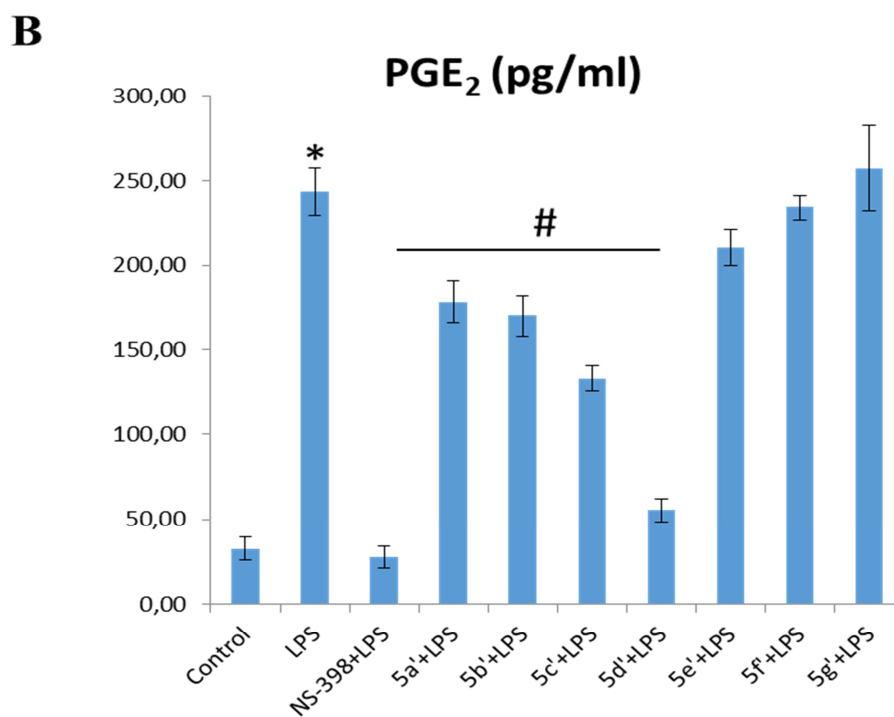
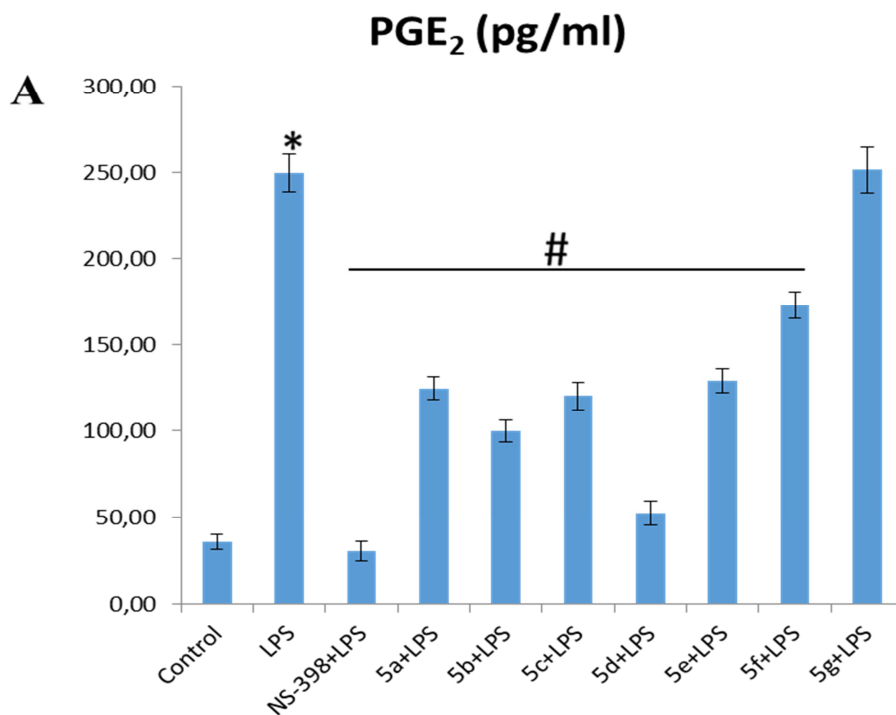


**Fig. 5.** Evaluation of COX-2 activity inhibition of synthesized analogues of cyclocoumarol **5a-g**, **5a'-5g'**. Synthesis of PGE<sub>2</sub> after pretreatment with pharmacological agents; nd: no determined, **A** with major diastereomers, **5a-g** **B** with minor diastereomers, **5a'-5g'**. PGE<sub>2</sub> production was measured in culture supernatants according to the manufacturer's instructions (PGE<sub>2</sub> EIA Kit, Cayman Chemical). Values are expressed as mean±SEM (\*P-value relative to control group, \* p<0.05; (#P-value relative to LPS group, #p<0.05).

Considering these results on PGE<sub>2</sub> production, we evaluated the dose-response behavior of the most active molecule **5d**. Four experiments at different concentrations were conducted at 1 μM, 5 μM, 10 μM and 20 μM using NS-398 as reference. At 1 μM, a low inhibition for **5d** (3%) and the reference NS-398 (11%) was noted. At 5 μM 45% and 61% of inhibition was observed for **5d** and NS-398 respectively. An activity comparable to NS-398 was observed at 10 μM and 20 μM with 79% and 89% of inhibition respectively. These results confirmed that the analogue **5d** displays a dose-dependent inhibition profile (Table 2, Fig. 6A). We then analyzed if the molecule **5d** had an effect on COX-2 expression. With regard to the dose-response used, we can say that the molecule **5d** does not modify the expression of COX-2 (Fig. 6B) but only its activity (Fig. 6A).

**Table 2** Inhibition of PGE<sub>2</sub> production stimulated by LPS by molecule **5d** in the Raw 264.7 cells at different doses.

Dose (μM)	% inhibition de PGE <sub>2</sub>	
	NS-398	<b>5d</b>
1	11	3
5	61	45
10	88	79
20	94	89

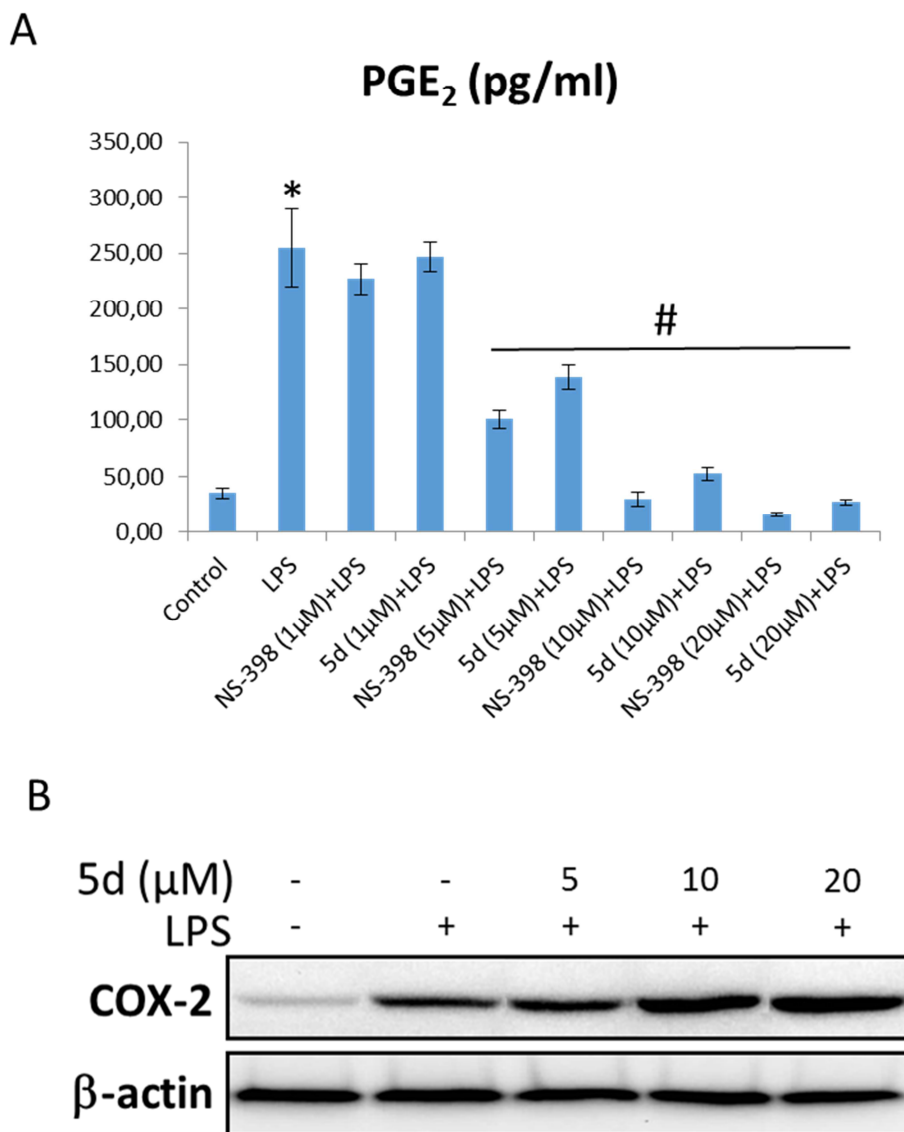
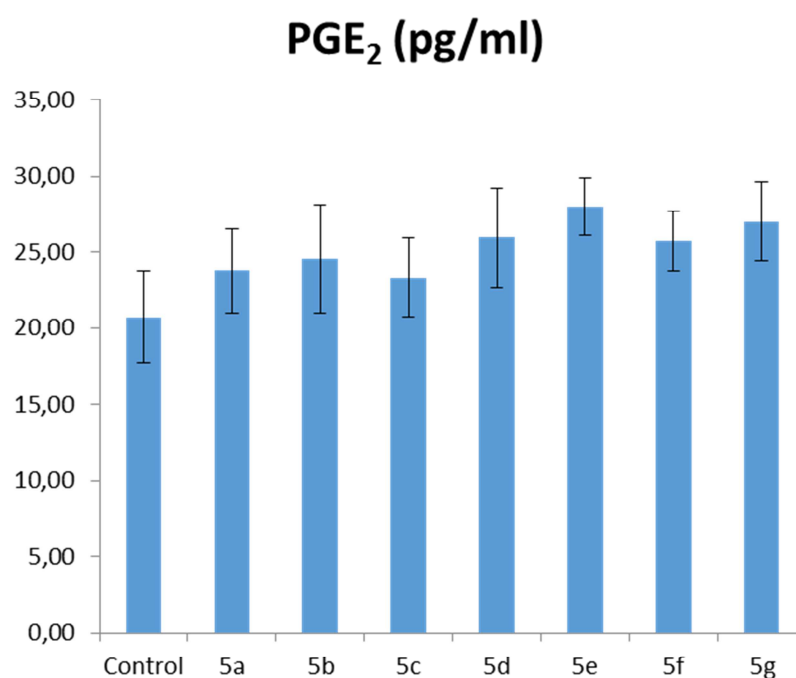


**Fig. 6.** Dose-response of **5d** compound of COX-2 activity (A) and expression (B) inhibition. (A) PGE<sub>2</sub> production was measured in culture supernatants according to the manufacturer's instructions (PGE<sub>2</sub> EIA Kit, Cayman Chemical). Values are expressed as mean±SEM (\*P-value relative to control group, \* p<0.05; (#P-value relative to LPS group, #p<0.05). (B) COX-2 expression was evaluated in the total cellular pool using Western blot analysis (β-actin was used as a loading control and the blot shown is representative of three separate experiments).

COX-2/COX-1 inhibition of majors diastereomers **5a-5g** was also studied to confirm the COX-2 selectivity. It has been extensively noted in the literature that non-selective molecules have side effects affecting especially the gastrointestinal system. The COX-1 activity inhibition assay was performed without LPS in the medium, measuring the production rate of PGE<sub>2</sub> synthesized by COX-1 (Fig. 7A). The effect of 10  $\mu$ M molecule **5d** on COX-1 expression was also analyzed (Fig. 7B).

A



B

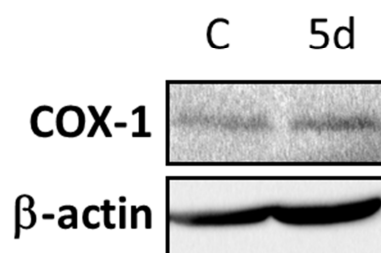


**Fig. 7.** Evaluation of COX-1 activity (A) and expression (B) inhibition of synthesized analogues of cyclocoumarol. (A) PGE<sub>2</sub> production was measured in culture supernatants according to the manufacturer's instructions (PGE<sub>2</sub> EIA Kit, Cayman Chemical). Values are expressed as mean $\pm$ SEM. (B) Raw 264.7 cells were treated or not (C, control) with 10  $\mu$ M molecule **5d** for 24 h. COX-1

expression was evaluated in the total cellular pool using Western blot analysis ( $\beta$ -actin was used as a loading control and the blot shown is representative of three separate experiments).

The results obtained in the *in vitro* COX-1/COX-2 inhibition study showed that synthesized molecules display no significant inhibition of COX-1 expression and activity (Fig. 7B and 7A respectively). This confirmed the previous results and identified compound **5d** as a selective inhibitor of COX-2 activity.

#### 2.4 Molecular modeling

To understand the ability of the synthesized compounds to inhibit COX-2 activity and to get some insights on their binding mode into the COX-2 binding site, the selected compounds were docked into the binding site of COX-2, defined using the co-crystallized selective COX-2 inhibitor as a reference, SC-558 (PDB ID: 1CX2). The choice of the PDB structure was based on a previous benchmarking study [12] in which the selected structure 1CX2 was associated with the highest performance in discriminating COX-2 inhibitors from decoy compounds [13], i.e. presumed inactive compounds. The predicted conformations of the ligand in the binding site were generated with the docking software AutoDock Vina and Surflex-dock that display different conformational search algorithms and different scoring functions. To validate our docking protocols with AutoDock VINA and Surflex-Dock, a preliminary re-docking study of the 1CX2 co-crystallized ligand, the selective COX-2 inhibitor SC-558, was performed in the 1CX2 active site. We were able to reproduce the experimental binding mode of the co-crystallized SC-558 with a RMSD (root mean square deviation) of 1.405 Å and of 1.067 Å with AutoDock VINA and Surflex-Dock respectively. We then performed the molecular docking of our synthesized cyclocoumarol analogues associated with the best and the worst PGE<sub>2</sub> inhibition potency (respectively compound **5d** and compound **5g**) to understand their structure-activity relationships. Both docking software predicted similar binding mode for compound **5d** with a RMSD value computed between AutoDock VINA and Surflex-Dock poses equal to 0.576 Å. As presented in Fig. 8, the coumarin scaffold of compound **5d** is predicted to be bound in the COX-2 binding site pocket formed by Met113,

Val116, Val349, Tyr355, Leu359 and Leu 531 [14] and stabilized through hydrogen bonds with Arg120 and Tyr355.

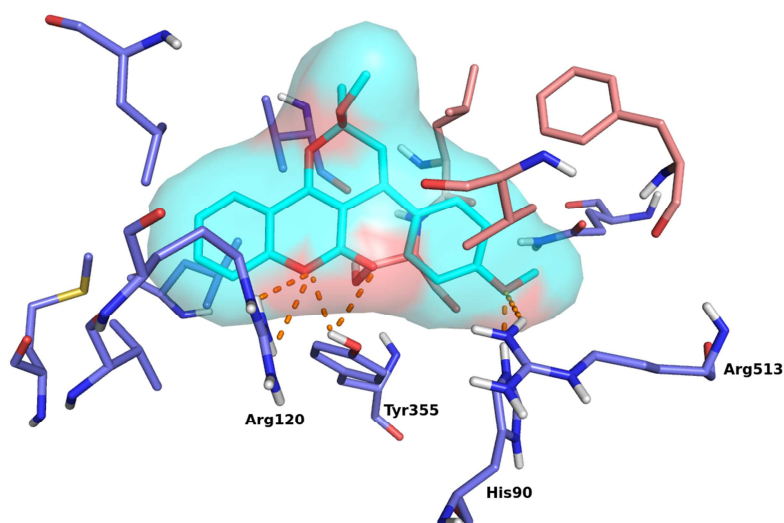


**Fig. 8.** Binding mode of compound **5d** in the binding site of COX-2.

The methoxybenzene moiety of compound **5d** is accommodated in a cavity that could not be observed in the COX-1 structure [14] and the oxygen atom of the methoxy group is linked by hydrogen bonds to His90 and Arg513. This ability to occupy the selective COX-2 cavity is a common feature of COX-2 selective inhibitors and could explain the COX-2 selectivity experimentally observed for compound **5d**. We re-scored the compound **5d** docking pose with the HYDE scoring function resulting in a predicted affinity in the  $\mu\text{M}$  to nM range (Fig. 9), consistent with experimental results (see Biological section).

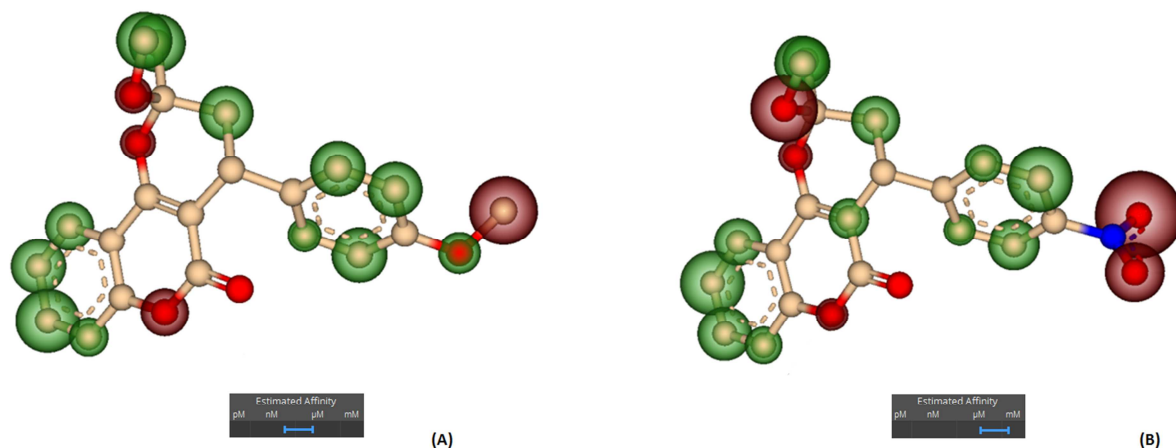


**Fig. 9.** Predicted affinity of compound **5d** (A) in the nM to  $\mu$ M range and of compound **5g** (B) in the  $\mu$ M to mM range using the HYDE scoring function implemented in SeeSAR.

We then explored the binding mode obtained for compound **5g** that displayed no PGE<sub>2</sub> inhibition potency in the biological experiments. The predicted binding mode of compound **5g** was very similar to the predicted binding mode of compound **5d** (Fig. 10).

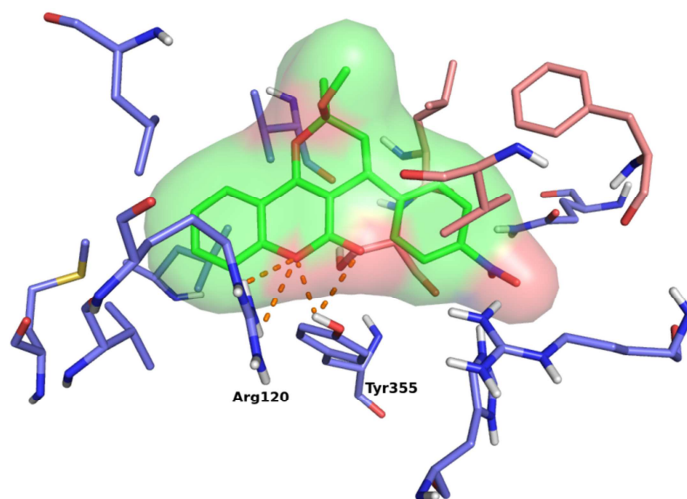


**Fig. 10.** Binding mode of compound **5g** in the binding site of COX-2.

The coumarin scaffold of compound **5g** is stabilized in the COX-2 binding site pocket formed by Met113, Val116, Val349, Tyr355, Leu359 and Leu 531 through hydrogen bonds with Arg120 and Tyr355 and the nitrobenzene moiety is oriented towards the COX-2 specific cavity [14]. However, nitro group are known to be weak hydrogen bond acceptors [15], and the additional hydrogen bond observed between compound **5d** and the COX-2 specific cavity could be lost with compound **5g** which could explain the loss of experimental activity. Re-scoring the compound **5g** docking pose with HYDE scoring function led to an estimated affinity in the range of mM to  $\mu$ M activity (Fig. 9), which is in accordance with the experimental results.

### 3. Conclusion

In summary, based on finding selective COX-2 inhibitors for inflammation treatment, a serie of novel cyclocoumarol derivatives was designed, synthesized, characterized and biologically evaluated. Most of

the synthesized compounds exhibited significant inhibitory activity on COX-2 without any significant inhibition on COX-1 activity. Among these, 2-methoxy-2-methyl-(1-(4-methoxyphenyl))-3,4-dihydropyrano[3,2-c]chromen-5(2H)-one, (compound **5d**), have showed the highest anti-inflammatory activity with a dose-dependent inhibition profile. The molecular modeling study allowed us to understand the inhibitory potential of synthesized compounds and suggested that the remarkable binding affinity of compound **5d** to COX-2 enzyme may be attributed to its ability to occupy a selective COX-2 cavity establishing additional hydrogen bonds between the oxygen of the methoxybenzene moiety and the His90 and Arg513 of the enzyme.

Our results revealed a new type of selective COX-2 inhibitors containing pyranocoumarin skeleton and proposed an interesting route towards the discovery of drugs with anti-inflammatory activities and may be a challenge in the research of COX-2 inhibitory therapy. The antiproliferative potential of the best compounds is currently being investigated and will be reported in due course.

### 3. Experimental section

#### 4.1. Chemistry

##### 4.1.1. General

All reagents were obtained from commercial sources unless otherwise noted, and used as received. Heated experiments were conducted using thermostatically controlled oil baths and were performed under an atmosphere oxygen-free in oven-dried glassware when necessary. All reactions were monitored by analytical Thin Layer Chromatography (TLC) and GC-MS analysis. TLC was performed on aluminium sheets precoated silica gel plates (60 F254, Merck). TLC plates were visualized using irradiation with light at 254 nm. Flash column chromatography was carried out when necessary using silica gel 60 (particle size 0.040-0.063 mm, Merck). Separation of diastereomers was performed on an Automate ISCO CombiFlash System RF75 PSI.

The structure of the products prepared by different methods was checked by comparison of NMR, IR and MS data and by the TLC behavior.  $^1\text{H}$  and  $^{13}\text{C}$ -NMR spectra were recorded on a Bruker BioSpin GmbH spectrometer 400 MHz, at room temperature. Chemical shifts are reported in  $\delta$  units, parts per

million (ppm). Coupling constants (J) are measured in hertz (Hz). Splitting patterns are designed as followed: s, singlet; d, doublet; dd, doublet of doublets; m, multiplet; br, broad; ddd: doublet of doublet of doublet. Various 2D techniques and DEPT experiments were used to establish the structures and to assign the signals. GC-MS analysis were performed with an Agilent 6890N instrument equipped with a dimethyl polysiloxane capillary column (12 m x 0.20 mm) and an Agilent 5973N MS detector-column temperature gradient 80-300°C (method 80): 80°C (1 min); 80°C to 300°C (12.05°C/min); 300°C (2 min); Infrared spectra were recorded over the 400-4000 cm<sup>-1</sup> range with an Agilent Technologies Cary 630 FTIR/ ATR/ ZnSe spectrometer.

Melting points were recorder on a Kofler hot block Heizbank type 7841 and were uncorrected. The reactions using microwaves as the activating/heating source were accomplished using a microwave oven (CEM Discover 1TM) under pressure and were monitored by ChemDriver.

X-ray diffraction data for compound **5a**, **5a'** and **5d** were obtained at room temperature on a Rigaku XtaLabPro diffractometer equipped with a microfocus source (MicroMax003\_Mo) and multilayer confocal mirrors (Mo K $\alpha$  radiation,  $\lambda = 0.71075 \text{ \AA}$ ). Data were indexed, integrated and scaled using CrysAlisPro [16] software suite. They were also corrected for polarization, Lorentz and absorption effects (SCALE3 ABSPACK).

The structure was solved with the ShelXT [17] structure solution program using Direct Methods and refined with the ShelXL [18] refinement package using Least Squares minimization. All non-hydrogen atoms were refined with anisotropic displacement parameters and C-bound H atoms have been added geometrically and treated as riding on their parent atoms. O-bound H atom was located in a difference Fourier and N-H distance was restrained to 0.87  $\text{\AA}$  using DFIX command and standard uncertainty (0.02  $\text{\AA}$ ).

High-resolution mass spectra (HRMS) analyses were acquired on a LTQ-Orbitrap XL from Thermo Scientific (Thermo Fisher Scientific, Courtaboeuf, France) mass spectrometer and operated in positive ionization mode, with a spray voltage at 3.6 kV. Detection was achieved in the Orbitrap with a resolution set to 60,000 (at m/z 400) and a m/z range between 110-1200 in profile mode. Spectrum was analyzed using the acquisition software XCalibur 2.1. The automatic gain control (AGC) allowed

accumulation of up to  $2 \cdot 10^5$  ions for FTMS scans, Maximum injection time was set to 300 ms and 1  $\mu$ scan was acquired. 5  $\mu$ L was injected using a Thermo Finnigan Surveyor HPLC system (Thermo Fisher Scientific, Courtaboeuf, France) with a continuous infusion of methanol at 100  $\mu$ L.min<sup>-1</sup>.

#### 4.1.2 Synthesis and characterization

Synthesis procedures of final compounds **5a-g** and **5a'-g'** are described below. All the experimental data and detailed attribution of the different <sup>1</sup>H and <sup>13</sup>C signals of compounds **4a-g** are available in the Supplementary material section.

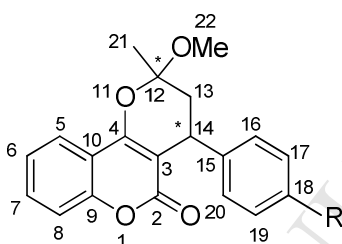


**Fig. 11.** Convention adopted to assign signals of <sup>1</sup>H and <sup>13</sup>C-NMR spectra

**4.1.2.1. 2-Methoxy-2-methyl-4-phenyl-3,4-dihydropyrano[3,2-c]chromen-5(2H)-one 5a.** Hydroxy-3-(3-oxo-1-phenylbutyl)-2H-chromen-2-one (1 equiv., 100 mg, 0.325 mmol, **4a**), was refluxed in HCl 4% MeOH (10 equiv., 3.25 mmol) for 23 h (monitoring by TLC, cyclohexane, AcOEt :7/3). Then the mixture was cooled down at room temperature and 1 mL of distilled water was added, followed by extraction with AcOEt. The diastereomers were separated by flash chromatography (eluent: cyclohexane/AcOEt : 8/2) and were isolated to afford 60 mg (53%) of the major diastereomer **5a** as a white powder and 10 mg (9%) of the minor diastereomer **5a'** as a white powder too. **5a**: *H14 in axial position*, *R<sub>f</sub>* = 0.33, cyclohexane/AcOEt : 8/2; Mp: 165-166°C; <sup>1</sup>H NMR (CDCl<sub>3</sub>, 300 MHz) :  $\delta$  (ppm): 1.70 (s, 3H, H21), 2.01 (dd, 1H, H13ax, *J*<sub>gem</sub> = 14.0 Hz, *J*<sub>13ax-14ax</sub> = 11.8 Hz ), 2.52 (dd, 1H, H13eq, *J*<sub>gem</sub> = 14.0 Hz, *J*<sub>eq-ax</sub> = 6.9 Hz ), 3.36 (s, 3H, H22), 4.16 (dd ,1H, H14ax, *J*<sub>ax-ax</sub> = 11.8 Hz, *J*<sub>ax-eq</sub> = 6.9 Hz ), 7.24-7.26 (m, 2H, H16, H20), 7.28-7.35 (m, 5H, H6, H8, H17, H18, H19), 7.53-7.58 (ddd, 1H ,H7, *J* = 9.4, 7.4, 1.7 Hz), 7.91 (dd, 1H ,H5, *J* = 8.0, 1.3 Hz). <sup>13</sup>C NMR (CDCl<sub>3</sub>, 75 MHz) :  $\delta$  (ppm): 22.35 (C21), 35.60 (C14), 43.52 (C13 ), 49.94 (C22), 101.44 (C3), 105.63 (C12), 115.80 (C10), 116.72 (C8), 122.46 (C5), 123.84 (C6), 126.54 (C18), 127.16 (C16, C20 or C17, C19), 128.72 (C17, C19 or

C16, C20), 131.62 (C7), 143.55 (C15), 153.14 (C9), 158.25 (C4), 161.19 (C2). NMR analysis are in agreement with literature [10] HRMS (ESI):  $m/z$  calcd. for  $C_{20}H_{18}O_4$   $[M+Na]^+$  : 345,1097; found : 345,1096. *Minor Diastereomer 5a'*: H14 in equatorial position  $R_f = 0.29$ , cyclohexane/AcOEt : 8/2;  $^1H$  NMR ( $CDCl_3$ , 300 MHz) :  $\delta$  (ppm): 1.69 (s, 3H, H21), 2.38 (dd, 1H, H13-ax,  $J_{gem} = 14.0$  Hz,  $J_{13ax-14eq} = 7.4$  Hz), 2.52 (dd, 1H, H13eq,  $J_{gem} = 14.1$  Hz,  $J_{13eq-eq} = 3.8$  Hz), 3.29 (s, 3H, H22), 4.19 (dd, 1H, H14eq,  $J_{eq-ax} = 7.2$  Hz,  $J_{eq-eq} = 3.7$  Hz), 7.21-7.32 (m, 5H, H16, H17, H18, H19, H20), 7.34-7.43 (m, 2H, H6, H8), 7.60-7.62 (m, 1H, H7), 7.96 (dd, 1H, H5,  $J = 7.8, 1.2$  Hz).  $^{13}C$  NMR ( $CDCl_3$ , 75 MHz) :  $\delta$  (ppm): 22.58 (C21), 35.45 (C14), 39.93 (C13), 49.41 (C22), 102.58 (C3), 103.30 (C12), 115.89 (C10), 116.86 (C8), 122.67 (C5), 123.97 (C6), 126.26 (C18), 127.52 (C16, C20 or C17, C19), 128.21 (C17, C19 or C16, C20), 131.87 (C7), 143.18 (C15), 153.11 (C9), 159.07 (C4), 162.00 (C2).

4.1.2.2. *2-Methoxy-2-methyl-(1-(p-tolyl))-3,4-dihydropyran[3,2-c]chromen-5(2H)-one 5b*. 4-hydroxy-3-(3-oxo-1-p-tolylbutyl)-2H-chromen-2-one (1 equiv., 100 mg, 0.31 mmol, **4b**), was refluxed in HCl 4% MeOH (10 equiv., 3.1 mmol) for 31 h (monitoring by TLC, cyclohexane, AcOEt : 7/3). Then the mixture was cooled down at room temperature and 1 mL of distilled water was added, followed by extraction with AcOEt. The diastereomers were separated by flash chromatography (eluent: cyclohexane/AcOEt : 8/2 and were isolated to afford 48 mg (46%) of the major diastereomer **5b** as a yellow powder and 13 mg (13%) of the minor diastereomer **5b'** as a yellow oil. **5b**:  $R_f = 0.42$ , cyclohexane/AcOEt : 8/2; Mp: 164-165°C;  $^1H$  NMR ( $CDCl_3$ , 300 MHz) :  $\delta$  (ppm): 1.82 (s, 3H, H21), 2.13 (t, 1H, H13ax,  $J_{gem} = 13.7$ ,  $J_{13ax-14ax} = 12.0$  Hz), 2.46 (s, 3H, H23), 2.62 (dd, 1H, H13eq,  $J_{gem} = 14.0$  Hz,  $J_{13eq-14ax} = 6.9$  Hz), 3.48 (s, 3H, H22), 4.24 (dd, 1H, H14-ax,  $J_{ax-ax} = 11.7$  Hz,  $J_{ax-eq} = 6.9$  Hz), 7.26 (m, 4H, H16, H17, H19, H20), 7.40-7.47 (m, 2H, H6, H8), 7.67 (t, 1H, H7,  $J = 7.6$  Hz), 8.03 (d, 1H, H5,  $J = 7.7$  Hz).  $^{13}C$  NMR ( $CDCl_3$ , 75 MHz) :  $\delta$  (ppm): 21.19 (C23), 22.35 (C21), 35.16 (C14), 43.58 (C13), 49.92 (C22), 101.43 (C3), 105.78 (C12), 115.82 (C10), 116.70 (C8), 122.44 (C5), 123.80 (C6), 127.01 (C16, C20 or C17, C19), 129.45 (C17, C19 or C16, C20), 131.56 (C7), 135.96 (C18), 140.47 (C15), 153.12 (C9), 158.15 (C4), 161.21 (C2). HRMS (ESI):  $m/z$  calcd. for  $C_{21}H_{20}O_4$

[M+Na]<sup>+</sup> : 359,1254 ; found : 359,1245 . **5b'**: Rf = 0.35, cyclohexane/AcOEt : 8/2; <sup>1</sup>H NMR (CDCl<sub>3</sub>, 300 MHz) : δ (ppm): 1.61 (s, 3H, H21), 2.48 (s, 3H, H23), 2.53-2.65 (m, 2H, H13ax , H13eq), 3.43 (s, 3H, H22), 4.27-4.30 (m, 4H, H16, H17, H19, H20), 7.48-7.55 (m, 2H, H6, H8), 7.74 (t, 1H, H7, *J* = 7.4 Hz), 8.08 (d, 1H, H5, *J* = 7.7 Hz). <sup>13</sup>C NMR (CDCl<sub>3</sub>, 75 MHz) : δ (ppm): 21.21 (C23 ), 22.59 (C21), 35.16 (C14), 40.05 (C13 ), 49.42 (C22), 102.57 (C3), 103.54 (C12), 115.79 (C10), 116.85 (C8), 122.65 (C5), 123.94 (C6), 127.38 (C16, C20 or C17, C19), 129.02 (C17, C19 or C16, C20), 131.81 (C7), 135.68 (C18), 140.18 (C15), 153.10 (C9), 158.96 (C4), 161.99 (C2).

4.1.2.3. *2-Methoxy-2-methyl-(1-(4-tert-butylphenyl)-3,4-dihydropyrano[3,2-c]chromen-5(2H)-one 5c*. 3-(1-(4-tert-butylphenyl)-3-oxobutyl)-4-hydroxy-2H-chromen-2-one (1 equiv., 100 mg, 0.27 mmol, **4c**), was refluxed in HCl 4% MeOH (10 equiv., 2.7 mmol) for 52 h (monitoring by TLC, cyclohexane, AcOEt :7/3). Then the mixture was cooled down at room temperature and 1 mL of distilled water was added, followed by extraction with AcOEt. The diastereomers were separated by flash chromatography (eluent: cyclohexane/AcOEt : 8/2 ) and were isolated to afford 55 mg (57%) of the major diastereomer **5c** as a white powder and 15 mg (16%) of the minor diastereomer **5c'** as a white powder too. **5c** : Rf = 0.48, cyclohexane/AcOEt : 8/2; Mp: 134-135°C ; <sup>1</sup>H NMR (CDCl<sub>3</sub>, 300 MHz) : δ (ppm): 1.26 (s, 9H, H23), 1.64 (s, 3H, H21), 1.96 (t, 1H, H13ax, *J*<sub>gem</sub> = *J*<sub>13ax-14ax</sub> = 13.8 Hz), 2.45 (dd, 1H, H13-eq, *J*<sub>gem</sub> = 14.0 Hz, *J*<sub>13eq-14ax</sub> = 7.0 Hz), 3.30 (s, 3H, H22), 4.07 (dd , 1H, H14ax, *J*<sub>ax-ax</sub> = 11.6 Hz, *J*<sub>ax-eq</sub> = 7.1 Hz ), 7.10-7.12 (m, 2H, H16, H20), 7.26-7.29 (m, 4H, H6 ,H8, H17, H19), 7.50 (t, 1H, H7, *J* = 7.7 Hz), 7.85 (d, 1H, H5, *J* = 8.3 Hz). <sup>13</sup>C NMR (CDCl<sub>3</sub>, 75 MHz) : δ (ppm): 22.36 (C21), 31.51 (C23), 35.07 (C14), 43.59 (C13), 49.92 (C22), 101.46 (C3), 105.87 (C12), 115.86 (C10), 116.70 (C8), 122.46 (C5), 123.80 (C6), 125.62 (C17, C19), 126.75 (C16, C20), 131.56 (C7), 140.32 (C15), 149.06 (C18), 153.12 (C9), 158.12 (C4), 161.23 (C2). HRMS (ESI): *m/z* calcd. for C<sub>24</sub>H<sub>26</sub>O<sub>4</sub> [M+Na]<sup>+</sup> : 401.1723; found: 401.1728, **5c'**: Rf = 0.39, cyclohexane/AcOEt : 8/2; <sup>1</sup>H NMR (CDCl<sub>3</sub>, 300 MHz) : δ (ppm): 1.28 (s, 9H, H23), 1.63 (s, 3H, H21), 2.29 (dd, 1H, H13-ax, *J*<sub>gem</sub> = 14.1 Hz, *J*<sub>13ax-14ax</sub> = 7.4 Hz), 2.45 (dd, 1H, H13eq, *J*<sub>gem</sub> = 14.0 Hz, *J*<sub>13eq-14eq</sub> = 4.1 Hz), 3.25 (s, 3H, H22), 4.10-4.12 (m, 1H, H14eq), 7.09-7.12 (m, 2H, H16, H20), 7.25-7.37 (m, 4H, H6 , H8, H17, H19), 7.56 (tb, 1H, H7, *J* = 7.3 Hz), 7.90 (d,

1H, H5,  $J = 7.8$  Hz).  $^{13}\text{C}$  NMR ( $\text{CDCl}_3$ , 75 MHz) :  $\delta$  (ppm): 22.56 (C21), 31.54 (C23), 35.18 (C14), 39.97 (C13), 49.46 (C22), 102.68 (C3), 103.61 (C12), 115.82 (C10), 116.83 (C8), 122.69 (C5), 123.93 (C6), 125.18 (C17, C19), 127.07 (C16, C20), 131.80 (C7), 139.98 (C15), 148.70 (C18), 153.09 (C9), 158.97 (C4), 162.00 (C2).

4.1.2.4. 2-Methoxy-2-methyl-(1-(4-methoxyphenyl))-3,4-dihydropyrano[3,2-c]chromen-5(2H)-one **5d**.

4-hydroxy-3-(1-(4-methoxyphenyl)-3-oxobutyl)-2H-chromen-2-one (1 equiv., 100 mg, 0.296 mmol, **4d**), was refluxed in HCl 4% MeOH (10 equiv., 1 g, 2.96 mmol) for 66 h (monitoring by TLC, cyclohexane, AcOEt :7/3). Then the mixture was cooled down at room temperature and 1 mL of distilled water was added, followed by extraction with AcOEt. The major diastereomer **5d** was purified by flash chromatography (eluent : cyclohexane/AcOEt : 8/2) and was isolated to afford 66 mg (63 %) as a white powder. **5d**: Rf = 0.39, cyclohexane/AcOEt : 8/2; Mp: 168 °C;  $^1\text{H}$  NMR ( $\text{CDCl}_3$ , 300 MHz) :  $\delta$  (ppm): 1.67 (s, 3H, H21), 1.96 (dd, 1H, H13ax,  $J_{\text{gem}} = 14.0$  Hz,  $J_{13\text{ax}-14\text{ax}} = 11.7$  Hz), 2.46 (dd, 1H, H13eq,  $J_{\text{gem}} = 14.0$  Hz,  $J_{13\text{eq}-14\text{ax}} = 7.0$  Hz), 3.33 (s, 3H, H22), 3.77 (s, 3H, H23), 4.08 (dd, 1H, H14ax,  $J_{\text{ax-ax}} = 11.9$  Hz,  $J_{\text{ax-eq}} = 7.2$  Hz), 6.82-6.85 (m, 2H, H17, H19), 7.13-7.16 (m, 2H, H16, H20), 7.26-7.32 (m, 2H, H6, H8), 7.53 (t, 1H, H7,  $J = 8.6$  Hz), 7.89 (d, 1H, H5,  $J = 6.7$  Hz).  $^{13}\text{C}$  NMR ( $\text{CDCl}_3$ , 75 MHz) :  $\delta$  (ppm): 22.36 (C21), 34.75 (C14), 43.56 (C13), 49.92 (C22), 55.31 (C23), 101.49 (C3), 105.86 (C12), 114.17 (C17, C19), 115.83 (C10), 116.70 (C8), 122.46 (C5), 123.81 (C6), 128.12 (C16, C20), 131.57 (C7), 135.46 (C15), 153.12 (C9), 158.08 (C18), 158.21 (C4), 161.20 (C2). HRMS (ESI): m/z calcd. for  $\text{C}_{21}\text{H}_{20}\text{O}_5$   $[\text{M}+\text{Na}]^+$  375,1203; found: 375,1203.

4.1.2.5. 2-Methoxy-2-methyl-(1-(4-fluorophenyl))-3,4-dihydropyrano[3,2-c]chromen-5(2H)-one **5e**.

3-(1-(4-fluorophenyl)-3-oxobutyl)-4-hydroxy-2H-chromen-2-one (1 equiv., 100 mg, 0.29 mmol, **4e**), was refluxed in HCl 4% MeOH (10 equiv., 2.90 mmol) for 31 h (monitoring by TLC, cyclohexane, AcOEt :7/3). Then the mixture was cooled down at room temperature and 1 mL of distilled water was added, followed by extraction with AcOEt. The diastereomers were separated by flash chromatography (eluent: cyclohexane/AcOEt : 8/2) and were isolated to afford 47 mg (44%) of the major diastereomer **5e** as a white powder and 21 mg (19%), of the minor diastereomer **5e'** as a yellow powder. **5e**: Rf = 0.34,

cyclohexane/AcOEt : 8/2; Mp: 164-166°C;  $^1\text{H}$  NMR ( $\text{CDCl}_3$ , 300 MHz) :  $\delta$  (ppm): 1.98 (s, 3H, H21), 2.24 (dd, 1H, H13ax,  $J_{\text{gem}} = 14.0$  Hz,  $J_{13\text{ax}-14\text{ax}} = 12$  Hz), 2.75 (dd, 1H, H13eq,  $J_{\text{gem}} = 14.0$  Hz,  $J_{13\text{eq}-14\text{ax}} = 6.9$  Hz), 3.62 (s, 3H, H22), 4.41 (dd, 1H, H14ax,  $J_{\text{ax-ax}} = 11.8$  Hz,  $J_{\text{ax-eq}} = 6.9$  Hz), 7.23-7.29 (m, 2H, H17, H19), 7.45-7.49 (m, 2H, H16, H20), 7.55-7.62 (m, 2H, H6, H8), 7.82 (m, 1H, H7), 8.17 (m, 1H, H5).  $^{13}\text{C}$  NMR ( $\text{CDCl}_3$ , 75 MHz) :  $\delta$  (ppm) : 22.31 (C21), 34.92 (C14), 43.50 (C13), 49.96 (C22), 101.45 (C3), 105.40 (C12), 115.51 (d, C17, C19,  $2J_{\text{C-F}} = 21.8$  Hz), 115.71 (C10), 116.72 (C8), 122.51 (C5), 123.92 (C6), 128.60 (d, C16, C20,  $3J_{\text{C-F}} = 8.3$  Hz), 131.74 (C7), 139.16 (C15), 153.12 (C9), 159.14 (d, C18,  $J_{\text{C-F}} = 120.8$  Hz), 161.17 (C4), 163.17 (C2). HRMS (ESI):  $m/z$  calcd. for  $\text{C}_{20}\text{H}_{17}\text{FO}_4$   $[\text{M}+\text{Na}]^+$  363,1003; found 363,1003. **5e**: Rf = 0.27, cyclohexane/AcOEt : 8/2;  $^1\text{H}$  NMR ( $\text{CDCl}_3$ , 300 MHz) :  $\delta$  (ppm): 1.96 (s, 3H, H21), 2.64 (dd, 1H, H13ax,  $J_{\text{gem}} = 14.1$  Hz,  $J_{13\text{ax}-14\text{eq}} = 7.3$  Hz), 2.75 (dd, 1H, H13eq,  $J_{\text{gem}} = 14.1$  Hz,  $J_{13\text{eq}-14\text{eq}} = 3.0$  Hz), 3.54 (s, 3H, H22), 4.45 (m, 1H, H14eq), 7.23-7.29 (m, 2H, H17, H19), 7.45-7.49 (m, 2H, H16, H20), 7.63-7.70 (m, 2H, H6, H8), 7.89 (t, 1H, H7,  $J = 7.3$  Hz), 8.23 (d, 1H, H5,  $J = 7.8$  Hz).  $^{13}\text{C}$  NMR ( $\text{CDCl}_3$ , 75 MHz) :  $\delta$  (ppm): 22.63 (C21), 34.57 (C14), 39.87 (C13), 49.38 (C22), 102.42 (C3), 103.12 (C12), 115.00 (d, C17, C19,  $2J_{\text{C-F}} = 21.8$  Hz), 115.65 (C10), 116.88 (C8), 122.68 (C5), 124.07 (C6), 129.0 (d, C16, C20,  $3J_{\text{C-F}} = 8.3$  Hz), 132.00 (C7), 138.87 (C15), 153.09 (C9), 159.42 (C18), 162.02 (C4), 163.01 (C2).

4.1.2.6. *2-Methoxy-2-methyl-(1-(4-trifluoromethyl)phenyl))-3,4-dihydropyrano[3,2-c]chromen-5(2H)-one* **5f**. 4-hydroxy-3-(3-oxo-1-(4-(trifluoromethyl)phenyl)butyl)-2H-chromen-2-one (1 equiv., 100 mg, 0.27 mmol, **4f**), was refluxed in HCl 4% MeOH (10 equiv, 2.7 mmol) for 23 h (monitoring by TLC, cyclohexane, AcOEt :7/3). Then the mixture was cooled down at room temperature and 1 mL of distilled water was added, followed by extraction with AcOEt. The diastereomers were separated by flash chromatography (eluent: cyclohexane/AcOEt : 8/2) and were isolated to afford 42 mg (38%) of the major diastereomer **5f** and 9 mg (8%) of the minor diastereomer **5f'** as a yellow powders. Mp: 180-182°C;  $^{13}\text{C}$  NMR ( $\text{CDCl}_3$ , 75 MHz) :  $\delta$  (ppm) = 22.32 (C21), 35.61 (C14), 43.26 (C13), 50.05 (C22), 101.40 (C3), 104.80 (C12), 115.66 (C10), 116.85 (C8), 122.56 (C5), 124.04 (C6), 128.8 (q, C18,  $2J_{\text{C-F}} = 32.2$  Hz), 125.75 (q, C17, C19,  $3J_{\text{C-F}} = 3.8$  Hz), 125.75 (C16, C20), 131.96 (C7), 147.86 (C15),

153.19 (C9), 158.72 (C4), 161.23 (C2), C23-F non visible. HRMS (ESI):  $m/z$  calcd. for  $C_{21}H_{17}F_3O_4$   $[M+Na]^+$  : 413,0971; found: 413,0980, **5f'**:  $R_f$  = 0.27, cyclohexane/AcOEt : 8/2:  $^1H$  NMR ( $CDCl_3$ , 300 MHz) :  $\delta$  (ppm): 1.65 (s, 3H, H21), 2.35 (dd, 1H, H13ax,  $J_{gem}$  = 14.2 Hz,  $J_{13ax-14eq}$  = 7.4 Hz), 2.48 (dd, 1H, H13-eq,  $J_{gem}$  = 14.2 Hz,  $J_{13eq-14eq}$  = 2.8 Hz), 3.19 (s, 3H, H22), 4.19 (m, 1H, H14-eq), 7.29 (d, 2H, H16, H20,  $J$  = 8.3 Hz ), 7.34-7.39 (m, 2H, H6, H8), 7.50 (d, 2H, H17, H19,  $J$  = 8.1 Hz ), 7.57 (td, 1H, H7,  $J$  = 7.4 Hz, 1.6 Hz), 7.92 (dd, 1H, H5,  $J$  = 7.9 Hz, 1.5 Hz).  $^{13}C$  NMR ( $CDCl_3$ , 75 MHz) :  $\delta$  (ppm): 22.62 (C21), 35.00 (C14), 39.60 (C13), 49.33 (C22 ), 102.30 (C3), 102.47 (C12), 115.57 (C10), 116.99 (C8), 122.71 (C5), 124.18 (C6), 125.15 (q, C17, C19,  $3J_{C-F}$  = 3.8 Hz), 128.00 (C16, C20), 132.19 (C7), 147.46 (C15), 153.17 (C9), 159.31 (C4), 162.07(C2), C18 et C23-F non visible.

4.1.2.7. *2-Methoxy-2-methyl-(1-(4-nitrophenyl))-3,4-dihydropyrano[3,2-c]chromen-5(2H)-one* **5g**. 4-hydroxy-3-(1-(4-nitrophenyl)-3-oxobutyl)-2H-chromen-2-one (1 equiv., 100 mg, 0.283 mmol, 8g), was refluxed in HCl 4% MeOH (10 equiv., 2.83 mmol) for 22 h (monitoring by TLC, cyclohexane, AcOEt : 7/3). Then the mixture was cooled down at room temperature and 1 mL of distilled water was added, followed by extraction with AcOEt. The diastereomers were separated by flash chromatography (eluent: cyclohexane/AcOEt : 8/2 ) and were isolated to afford 63 mg (64%) of the major diastereomer **7g** as a white powder and 11 mg (12%) of the minor diastereomer **7g'** as a yellow powder. **7g**:  $R_f$  = 0.24, cyclohexane/AcOEt : 8/2; Mp: 204-206°C;  $^1H$  NMR ( $CDCl_3$ , 300 MHz) :  $\delta$  (ppm): 1.56 (s, 3H, H21), 1.95 (dd, 1H, H13ax,  $J_{gem}$  = 13.9 Hz,  $J_{13ax-14ax}$  = 12.1 Hz), 2.48 (dd, 1H, H13eq,  $J_{gem}$  = 13.9 Hz,  $J_{13eq-14ax}$  = 6.8 Hz), 3.35 (s, 3H, H22), 4.24 (dd ,1H, H14-ax,  $J_{ax-ax}$  = 12.1 Hz,  $J_{ax-eq}$  = 6.8 Hz ), 7.30-7.35 (m, 2H, H6, H8), 7.38 (d, 2H, H16, H20,  $J$  = 8.8 Hz), 7.57 (ddd, 1H, H7 ,  $J$  = 9.4 Hz, 7.3 Hz, 1.6 Hz), 7.89 (dd, 1H, H5,  $J$  = 9.7 Hz, 1.3 Hz), 8.16 (d, 2H, H17, H19,  $J$  = 8.8 Hz ).  $^{13}C$  NMR ( $CDCl_3$ , 75 MHz) :  $\delta$  (ppm): 22.31 (C21), 35.72 (C14), 42.91 (C13), 50.11 (C22), 101.36 (C3), 104.29 (C12), 115.54 (C10), 116.90 (C8), 122.60 (C5), 124.15 (C6 ,C17, C19), 128.11 (C16, C20), 132.16 (C7), 146.79 (C18), 151.65 (C15), 153.20 (C9), 158.95 (C4), 161.21(C2). HRMS (ESI):  $m/z$  calcd. for  $C_{20}H_{17}NO_6$   $[M+Na]^+$ : 390,0948; found: 390,0950. **7g'**:  $R_f$  = 0.16, cyclohexane/AcOEt : 8/2;  $^1H$  NMR ( $CDCl_3$ , 300 MHz) :  $\delta$  (ppm): 1.66 (s, 3H, H21), 2.37 (dd, 1H, H13ax,  $J_{gem}$  = 14.2 Hz,  $J_{13ax-14eq}$  =

7.4 Hz), 2.50 (dd, 1H, H13eq,  $J_{gem} = 14.2$  Hz,  $J_{13eq-14eq} = 2.5$  Hz), 3.17 (s, 3H, H22), 4.22 (dd, 1H, H14eq,  $J_{eq-ax} = 7.3$  Hz,  $J_{eq-eq} = 2.5$  Hz), 7.34 (d, 2H, H16, H20,  $J = 8.4$  Hz), 7.38-7.41 (m, 2H, H6, H8), 7.61 (ddd, 1H, H7,  $J = 9.2, 7.3, 1.6$  Hz), 7.92 (dd, 1H, H5,  $J = 7.9$  Hz, 1.5 Hz), 8.13 (d, 2H, H17, H19,  $J = 8.8$  Hz).  $^{13}\text{C}$  NMR ( $\text{CDCl}_3$ , 75 MHz) :  $\delta$  (ppm): 22.61 (C21), 34.92 (C14), 39.45 (C13), 49.32 (C22), 101.94 (C3), 102.18 (C12), 116.06 (C10), 117.06 (C8), 122.75 (C5), 123.46 (C17, C19), 124.30 (C6), 128.54 (C16, C20), 132.40 (C7), 146.43 (C18), 151.29 (C15), 153.18 (C9), 159.12 (C4), 162.10 (C2).

#### 4.1.3 X-ray analysis

The crystallographic analysis of 2-methoxy-2-methyl-4-phenyl-3,4-dihydropyrano[3,2-c]chromen-5(2H)-one **5a**, **5a'** and 2-methoxy-2-methyl-(1-(4-methoxyphenyl))-3,4-dihydropyrano[3,2-c]chromen-5(2H)-one **5d** are described below. The complete characterization containing the crystal data and structure refinement is available in the Supplementary material section.

The relative configuration of 2-methoxy-2-methyl-4-phenyl-3,4-dihydropyrano[3,2-c]chromen-5(2H)-one **5a** was characterized as (S, S) and (R, R). **Crystal Data** for **5a** ( $M = 322.34$  g/mol): monoclinic, space group  $P2_1/n$  (no. 14),  $a = 5.8669(3)$  Å,  $b = 16.7563(8)$  Å,  $c = 16.4159(9)$  Å,  $\beta = 94.830(5)^\circ$ ,  $V = 1608.08(15)$  Å<sup>3</sup>,  $Z = 4$ ,  $T = 292.7(5)$  K,  $\mu(\text{MoK}\alpha) = 0.092$  mm<sup>-1</sup>,  $D_{\text{calc}} = 1.331$  g/cm<sup>3</sup>, 16505 reflections measured ( $6.962^\circ \leq 2\theta \leq 60.034^\circ$ ), 4107 unique ( $R_{\text{int}} = 0.0458$ ,  $R_{\text{sigma}} = 0.0464$ ) which were used in all calculations. The final  $R_1$  was 0.0478 ( $I > 2\sigma(I)$ ) and  $wR_2$  was 0.1397 (all data) (Fig. 12).

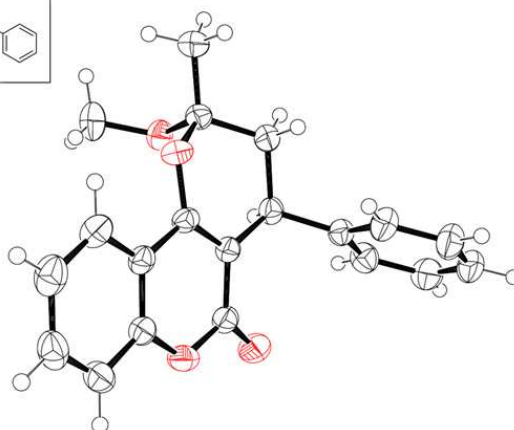
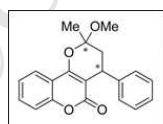


**Fig.12.** ORTEP-3 plot of major diastereomer **5a**. Ellipsoids are drawn at the 50% probability level and H atoms are shown as spheres of arbitrary radius.

The relative configuration of 2-methoxy-2-methyl-4-phenyl-3,4-dihydropyrano[3,2-c]chromen-5(2H)-one **5a'** was characterized as (S, R) and (R, S). **Crystal Data** for **5a'** (M = 322.34 g/mol): monoclinic, space group I2/a (no. 15), a = 20.1207(12) Å, b = 8.5036(4) Å, c = 19.9586(14) Å,  $\beta = 107.014(7)^\circ$ , V = 3265.5(4) Å<sup>3</sup>, Z = 8, T = 292.6(4) K,  $\mu(\text{MoK}\alpha) = 0.091 \text{ mm}^{-1}$ , D<sub>calc</sub> = 1.311 g/cm<sup>3</sup>, 18115 reflections measured ( $7.124^\circ \leq 2\theta \leq 60.164^\circ$ ), 4158 unique ( $R_{\text{int}} = 0.0587$ ,  $R_{\text{sigma}} = 0.0579$ ) which were used in all calculations. The final  $R_1$  was 0.0549 ( $I > 2\sigma(I)$ ) and  $wR_2$  was 0.1328 (all data) (Fig. 13).

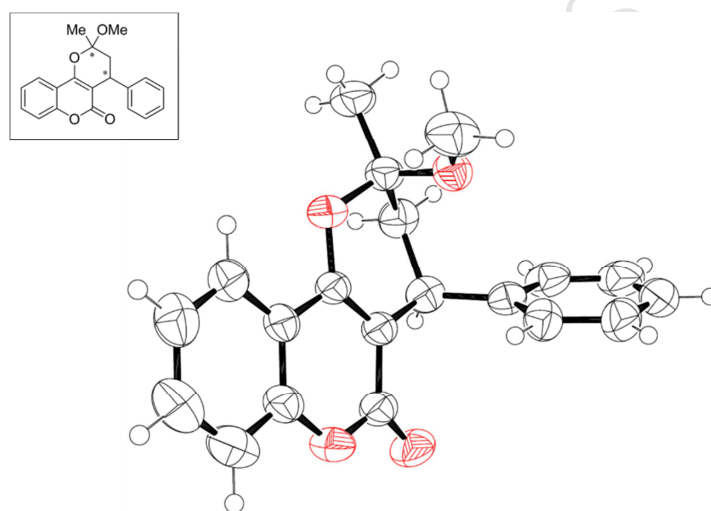


**Fig. 13.** ORTEP-3 plot of **5a'**. Ellipsoids are drawn at the 50% probability level and H atoms are shown as spheres of arbitrary radius.

The relative configuration of the 2-methoxy-2-methyl-(1-(4-methoxyphenyl))-3,4-dihydropyrano[3,2-c]chromen-5(2H)-one (**5d**), major diastereomer was characterized as (S, S) and (R, R). **Crystal Data** for **5d** (M = 352.37 g/mol): monoclinic, space group C2/c (no. 15), a = 23.694(2) Å, b = 5.6932(4) Å, c = 26.775(3) Å,  $\beta = 102.720(9)^\circ$ , V = 3523.2(6) Å<sup>3</sup>, Z = 8, T = 292.5(7) K,  $\mu(\text{MoK}\alpha) = 0.095 \text{ mm}^{-1}$ , D<sub>calc</sub> = 1.329 g/cm<sup>3</sup>, 19052 reflections measured ( $7.372^\circ \leq 2\theta \leq 59.93^\circ$ ), 4454 unique ( $R_{\text{int}} = 0.0552$ ,  $R_{\text{sigma}} = 0.0590$ ) which were used in all calculations. The final  $R_1$  was 0.0490 ( $I > 2\sigma(I)$ ) and  $wR_2$  was 0.1362 (all data) (Fig. 14).

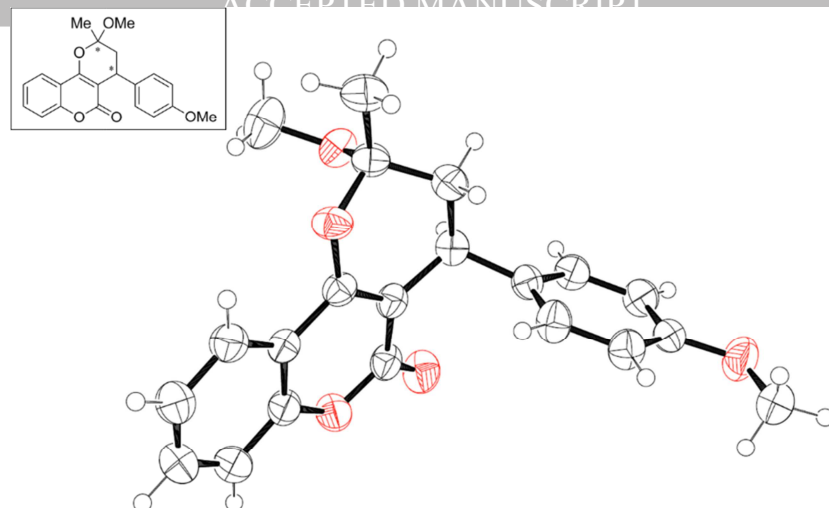


**Fig. 14.** ORTEP-3 plot of **5d**. Ellipsoids are drawn at the 50% probability level and H atoms are shown as spheres of arbitrary radius.

Crystallographic data for 2-methoxy-2-methyl-4-phenyl-3,4-dihydropyrano[3,2-c]chromen-5(2H)-one **5a** and **5a'** and 2-methoxy-2-methyl-(1-(4-methoxyphenyl))-3,4-dihydropyrano[3,2-c]chromen-5(2H)-one **5d**, have been deposited with the Cambridge Crystallographic Data Centre (deposit no. CCDC 1563254-1563256). Copies of the data can be obtained, free of charge, from The Cambridge Crystallographic Data Centre via [www.ccdc.cam.ac.uk/data\\_request/cif](http://www.ccdc.cam.ac.uk/data_request/cif).

#### 4.1.4 Biology

##### 4.1.4.1. Assay of COX-2 activity

Raw 264.7 murine macrophages (ATCC TIB 71; American Type Culture Collection, Rockville, MD, USA) were maintained in DMEM supplemented with 10% (v/v) heat-inactivated fetal calf serum, 100 U/mL penicillin and 100 µg/mL streptomycin. The cells were grown in a humidified incubator at 37 °C and 5% CO<sub>2</sub>. Raw 264.7 cells were seeded at 2.10<sup>5</sup> cells/well during 24 h, then 10 µM of each synthesized cyclocoumarol derivatives was added. After 2 h, LPS (10 ng/mL) was added in the culture medium during 24 h. The PGE<sub>2</sub> levels were quantified in culture media supernatants from treated and control cells by enzyme immunoassay using an EIA Kit (Cayman Chemical) as previously described

[19]. The results were expressed by the standard deviation average of  $\pm 8$  independent experiments. NS-398, a well-known COX-2 selective inhibitor was used as reference.

#### 4.1.4.2. Assay of COX-1 activity

The same protocol described before was used except for the absence of LPS and deprivation of SVF (1%) to measure the COX-1 activity. The PGE<sub>2</sub> levels were quantified in culture media supernatants from treated and control cells by enzyme immunoassay using an EIA Kit (Cayman Chemical). The results were expressed by the standard deviation average of  $\pm 6$  independent experiments.

#### 4.1.4.3 Assay of dose-dependent response for compound 5d

The same protocol described in Assay of COX-2 activity section was used except for the concentration of the molecules (1-20  $\mu$ M). The PGE<sub>2</sub> levels were quantified in culture media supernatants from treated and control cells by enzyme immunoassay using an EIA Kit (Cayman Chemical). The results were expressed by the standard deviation average of  $\pm 6$  independent experiments.

#### 4.1.4.4. Protein extraction and Western-Blot analysis

For total protein extraction, Raw 264.7 cells were washed in PBS, then, the total cell pool was centrifuged at 200 g for 5 min at 4°C and homogenized in RIPA lysis buffer (50 mM HEPES, pH 7.5, 150 mM NaCl, 1% sodium deoxycholate, 1% NP-40, 0.1% SDS, 20 mg/mL of aprotinin) containing protease inhibitors (Complete™ Mini, Roche Diagnostics) according to the manufacturer's instructions. Proteins (10-100  $\mu$ g) were separated by electrophoresis on 10% SDS-PAGE gels and transferred to polyvinylidene fluoride (PVDF) membranes (Amersham Pharmacia Biotech, Saclay, France) and probed with human primary antibodies. Human COX-1 and COX-2 antibodies were purchased from Cayman Chemical (Bertin Pharma, Montigny le Bretonneux, France). After incubation with secondary antibodies (Dako France S.A.S., Trappes, France), blots were developed using the ECL Plus Western Blotting Detection System (Amersham Pharmacia Biotech) and G: BOX system (Syngene,

Ozyme, Saint Quentin en Yvelines, France). Membranes were then reblotted with human anti- $\beta$ -actin (Sigma Aldrich, Saint Quentin Fallavier, France) used as a loading control.

#### 4.1.5. Molecular modeling study

Coordinates of *Mus musculus* COX-2 in complex with a selective COX-2 inhibitor, SC-558, were retrieved from the X-ray structure available in the Protein Data Bank (PDB) [20] (accession code 1CX2, resolution 3.0 Å). Only chain A was retained. The ligand bound in the active site was removed and the protein structure was prepared for docking studies using the DockPrep tool of UCSF CHIMERA [21] to delete the co-crystallized water molecules, repair truncated side chains, protonate the protein residues and assign atomic partial charges using the AMBER force field ff14SB [22]. The 3D structures of compounds **5a-g** were generated with Corina online demo [23]. OpenBabel [24] was used to calculate Gasteiger's partial atomic charges. Compounds **5a-g** were then docked individually using AutoDock VINA [25] with default parameters. To confirm the predicted docking poses obtained with AutoDock VINA, we used Surflex-Dock v. 2.5 [26], with the +premin and +remin options. SeeSAR v6.0 [27] was then used to re-score the docked poses using the HYDE scoring function [28].

#### 4.1.6. Statistical analysis

Data are expressed as the arithmetic means  $\pm$  standard error of the mean (SEM) of separate experiments. The statistical significance of results obtained from *in vitro* studies was evaluated by the two tailed unpaired Student's t-test, with  $p < 0.05$  being considered as significant.

#### Acknowledgements

The authors acknowledge the Ministry of National Education, Research and Technology (MENRT) for the graduate fellowship awarded to Anita Rayar. Authors also thank Pr Marie-Claude Viaud-Massuard and Dr Cécile Croix for their help in the use of the CombiFlash system. The authors would like to thank Pr Ajay Jain for providing Surflex and BiosolveIT GmbH for providing SeeSAR.

**Supplementary data**

Supplementary data related to this article can be found <http://dx.doi.org/XX.XXXX/j.ejmech.2017.XX.XXX>

**References**

- [1] F. Celotti, S. Laufer, Anti-inflammatory drugs: new multitarget compounds to face an old problem. The dual inhibition concept, *Pharmacol. Res.* 43 (2001) 429-436.
- [2] A.L. Blobaum, L.J. Marnett, Structural and Functional Basis of Cyclooxygenase Inhibition, *J. Med. Chem.* 50 (2007) 1425-1441.
- [3] D.L. Simmons, R.M. Botting, T. Hla, Cyclooxygenase Isozymes: The Biology of Prostaglandin Synthesis and Inhibition, *Pharmacol. Rev.* 56 (2004) 387.
- [4] S. Harirforoosh, W. Asghar, F. Jamali, Adverse effects of nonsteroidal antiinflammatory drugs: An update of gastrointestinal, cardiovascular and renal complications, *J. Pharm. Pharma. Sci.* 16 (2013) 821-847.
- [5] A.-M. Rayar, N. Lagarde, C. Ferroud, J.-F. Zagury, M. Montes, M. Sylla-Iyarreta Veitía, Update on COX-2 Selective Inhibitors: Chemical Classification, Side Effects and their Use in Cancers and Neuronal Diseases, *Curr. Top. Med. Chem.* 17 (2017) 1-22.
- [6] M. Sylla-Iyarreta Veitía, D. Siverio Mota, V. Lerari, M. Marín, R. M. Giner, L. Vicet Muro, Y. Rivero Guerra, F. Dumas, C. Ferroud, P. A. M. de Witte, A. D. Crawford, V. J. Arán, Y. Marrero Ponce, Fishing Anti-Inflammatories from Known Drugs: In Silico Repurposing, Design, Synthesis and Biological Evaluation of Bisacodyl Analogues, *Curr. Top. Med. Chem.* 17 (2017). 2866 - 2887.
- [7] A. Rayar, M.S.-I. Veitia, C. Ferroud, An efficient and selective microwave-assisted Claisen-Schmidt reaction for the synthesis of functionalized benzalacetones, *SpringerPlus* 4 (2015) 221.
- [8] M. Ikawa, M.A. Stahmann, K.P. Link, Studies on 4-Hydroxycoumarins. V. The Condensation of  $\alpha,\beta$ -Unsaturated Ketones with 4-Hydroxycoumarin1, *J. Am. Chem. Soc.* 66 (1944) 902-906.
- [9] W.M. Barker, M.A. Hermodson, K.P. Link, 4-Hydroxycoumarins. Synthesis of the metabolites and some other derivatives of warfarin, *J. Med. Chem.* 14 (1971) 167-169.

- [10] E.J. Valente, E.C. Lingafelter, W.R. Porter, W.F. Trager, Structure of warfarin in solution, *J. Med. Chem.* 20 (1977) 1489-1493.
- [11] L. Hassan, A. Pinon, Y. Limami, J. Seeman, C. Fidanzi-Dugas, F. Martin, B. Badran, A. Simon, B. Liagre, Resistance to ursolic acid-induced apoptosis through involvement of melanogenesis and COX-2/PGE2 pathways in human M4Beu melanoma cancer cells, *Exp. Cell Res.* 345 (2016) 60-69.
- [12] N. Ben Nasr, H. Guillemain, N. Lagarde, J.F. Zagury, M. Montes, Multiple structures for virtual ligand screening: defining binding site properties-based criteria to optimize the selection of the query, *J. Chem. Inf. Model.* 53 (2013) 293-311.
- [13] N. Huang, B.K. Shoichet, J.J. Irwin, Benchmarking sets for molecular docking, *J. Med. Chem.* 49 (2006) 6789-6801.
- [14] R.G. Kurumbail, A.M. Stevens, J.K. Gierse, J.J. McDonald, R.A. Stegeman, J.Y. Pak, D. Gildehaus, J.M. Miyashiro, T.D. Penning, K. Seibert, P.C. Isakson, W.C. Stallings, Structural basis for selective inhibition of cyclooxygenase-2 by anti-inflammatory agents, *Nature* 384 (1996) 644-648.
- [15] W.F. Baitinger, P.v.R. Schleyer, T.S.S.R. Murty, L. Robinson, Nitro groups as proton acceptors in hydrogen bonding, *Tetrahedron* 20 (1964) 1635-1647.
- [16] C.S.s. Rigaku Oxford Diffraction, version 38.41o, Rigaku Corporation, Oxford, UK., (2015).
- [17] G.M. Sheldrick, SHELXT- Integrated space-group and crystal-structure determination, *Acta Crystallogr. Sect. A, Foundations and Advances* 71 (2015) 3-8.
- [18] G.M. Sheldrick, Crystal structure refinement with SHELXL, *Acta Crystallogr. Sect. C, Struct. Chem.* 71 (2015) 3-8.
- [19] C. Fidanzi-Dugas, B. Liagre, G. Chemin, A. Perraud, C. Carrion, C.Y. Couquet, R. Granet, V. Sol, D.Y. Léger, Analysis of the in Vitro and in Vivo Effects of Photodynamic Therapy on Prostate Cancer by Using New Photosensitizers, Protoporphyrin IX-polyamine Derivatives, *Biochim. Biophys. Acta* 1861 (2017) 1676-1690.
- [20] H.M. Berman, T. Battistuz, T.N. Bhat, W.F. Bluhm, P.E. Bourne, K. Burkhardt, Z. Feng, G.L. Gilliland, L. Iype, S. Jain, P. Fagan, J. Marvin, D. Padilla, V. Ravichandran, B. Schneider, N. Thanki, H. Weissig, J.D. Westbrook, C. Zardecki, The Protein Data Bank, *Act. Crystallogr. Sect. D, Biol. Crystallogr.* 58 (2002) 899-907.

- [21] E.F. Pettersen, T.D. Goddard, C.C. Huang, G.S. Couch, D.M. Greenblatt, E.C. Meng, T.E. Ferrin, UCSF Chimera--a visualization system for exploratory research and analysis, *J. Comput. Chem.* 25 (2004) 1605-1612.
- [22] J.A. Maier, C. Martinez, K. Kasavajhala, L. Wickstrom, K.E. Hauser, C. Simmerling, ff14SB: Improving the Accuracy of Protein Side Chain and Backbone Parameters from ff99SB, *J. Chem. Theory Comput.* 11 (2015) 3696-3713.
- [23] J. Sadowski, J. Gasteiger, G. Klebe, Comparison of Automatic Three-Dimensional Model Builders Using 639 X-Ray Structures, *J. Chem. Inform. Comput. Sci.* 34 (1994) 1000-1008.
- [24] N.M. O'Boyle, M. Banck, C.A. James, C. Morley, T. Vandermeersch, G.R. Hutchison, Open Babel: An open chemical toolbox, *J. Cheminform.* 3 (2011) 33.
- [25] O. Trott, A.J. Olson, AutoDock Vina: improving the speed and accuracy of docking with a new scoring function, efficient optimization, and multithreading, *J. Comput. Chem.* 31 (2010) 455-461.
- [26] A.N. Jain, Surflex: fully automatic flexible molecular docking using a molecular similarity-based search engine, *J. Med. Chem.* 46 (2003) 499-511.
- [27] A. Temirak, Y.M. Shaker, F.A.F. Ragab, M.M. Ali, H.I. Ali, H.I. El Diwani, Part I. Synthesis, biological evaluation and docking studies of new 2-furylbenzimidazoles as antiangiogenic agents, *Eur. J. Med. Chem.* 87 (2014) 868-880.
- [28] N. Schneider, G. Lange, S. Hindle, R. Klein, M. Rarey, A consistent description of HYdrogen bond and DEhydration energies in protein-ligand complexes: methods behind the HYDE scoring function, *J. Comput. Aided Mol. Des.* 27 (2013) 15-29.

## Highlights

### **New selective cyclooxygenase-2 inhibitors from cyclocoumarol: synthesis, characterization, biological evaluation and molecular modeling**

Anita Rayar <sup>a, b</sup>, Nathalie Lagarde <sup>b</sup>, Frederique Martin<sup>c</sup>, Florent Blanchard<sup>d</sup>, Bertrand Liagre <sup>c</sup>, Clotilde Ferroud <sup>a</sup>, Jean-François Zagury <sup>b</sup>, Matthieu Montes <sup>b</sup>, Maité Sylla-Iyarreta Veitia<sup>a\*</sup>

Corresponding author:

*E-mail address* : [maite.sylla@lecnam.net](mailto:maite.sylla@lecnam.net) (M. Sylla-Iyarreta Veitia)

- A new type of selective COX-2 inhibitors containing pyranocoumarin skeleton is proposed.
- The synthesized compounds exhibited no significant inhibition on COX-1.
- The additional hydrogen bonds in the selective COX-2 cavity may be responsible of the outstanding binding affinity.